Heliyon 9 (2023) e22183

Contents lists available at ScienceDirect

Heliyon

journal homepage: www.cell.com/heliyon

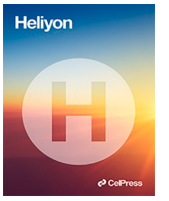

Formation of morpholine-acetamide derivatives as potent anti-tumor drug candidates: Pharmacological evaluation and molecular docking studies

Ahmed Sadiq Sheikh [a], Reem Altaf [c], Humaira Nadeem [a,*], Muhammad Tariq Khan [b], Babar Murtaza [a]

[a] Department of Pharmaceutical Chemistry, Riphah Institute of Pharmaceutical Sciences, RIU, Islamabad, Pakistan
[b] Faculty of Pharmacy, CUST, Islamabad, Pakistan
[c] Department of Pharmacy, Iqra University, Islamabad, Pakistan

ARTICLE INFO

Keywords:
Heterocyclic amines
Morpholine based compounds
Anti-tumor activity
MTT (3-[4,5-dimethylthiazole-2-yl]-2,5 diphenyl tetrazolium bromide) assay
Carbonic anhydrase inhibition
HIF-1α

ABSTRACT

Heterocyclic amines and acetamide derivatives are known for their chemotherapeutic potential. Hence, in the present study, morpholine was taken as a principal product and novel morpholine derivatives were designed, formulated, characterized, and screened for the mechanism of inhibition of carbonic anhydrase and their anticancer potential. In addition, *in vitro* inhibition of hypoxia-inducible factor-1 (HIF-1) protein was also investigated. Results revealed that compounds **1c, 1d,** and **1h** possessed significant inhibitory activities against carbonic anhydrase with IC_{50} of 8.80, 11.13, and 8.12 μM, respectively. Interestingly, the carbonic anhydrase inhibitory activity of compound **1h** was comparable with that of standard acetazolamide (IC_{50} 7.51 μM). The compounds **1h** and **1i** significantly inhibited the proliferation of ovarian cancer cell line ID8 with IC_{50} of 9.40, and 11.2 μM, respectively while the standard cisplatin exhibited an IC_{50} 8.50 μM. In addition, compounds **1c, 1b, 1h** and **1i** also exhibited significant inhibitory effects on HIF-1α. In conclusion, we report first time the biological potential of morpholine based compounds against ovarian cancer and HIF-1α that may serve as lead molecules for drug discovery.

1. Introduction

Cancer still has the second highest mortality rates on global level despite advances of therapeutics. The disease is characterized by uncontrolled cell growth creating tumors having potential to metastasize [1]. Uncontrolled rapidly dividing cells create demand for more oxygen supply that leads to hypoxic conditions within micro environment of tumor cell and stabilization of such micro environment is associated with the amplification of CA enzymes [2–5], especially isozymes Carbonic anhydrase IX/XII. Carbonic anhydrase (CA) is a zinc-containing cytoplasmic ubiquitous metalloenzyme that possess 16 distinct isozymes including membrane-bound isozymes, mitochondrial isozymes and salivary isozymes [6]. The enzyme is involved in catalytic conversion of water and CO_2 into bicarbonates and protons. Several physical and anatomical ailments are attributed to the upregulation of CA making it a valuable drug target. Unlike other CA isozymes, CA IX overexpression is a feature of certain physiological conditions like hypoxic tumors and related

* Corresponding author. Department of Pharmaceutical Chemistry, Riphah Institute of Pharmaceutical Sciences, Riphah International University, Islamabad, 440000, Pakistan.
E-mail address: humaira.nadeem@riphah.edu.pk (H. Nadeem).

https://doi.org/10.1016/j.heliyon.2023.e22183
Received 16 June 2023; Received in revised form 31 October 2023; Accepted 6 November 2023
Available online 14 November 2023

malignancies [7–10]. Several types of solid tumors are characterized by hypoxia due to inadequate vascular supply. To combat this situation, the tumor cells adopt several mechanisms including hypoxia-inducible factor (HIF) pathway. Hypoxia induced HIF stabilization enhances the production of zinc-containing dimeric glycoprotein carbonic anhydrase IX (CAIX) [11], which makes it an attractive drug target for anticancer therapies based on newly designed inhibitors. Human carbonic anhydrase (hCA) enzyme are being targeted for the management of several diseases [12–14]. The interactions of hCA inhibitors with the enzyme's catalytic region are well understood. The most common classical inhibitor of hCA is sulfonamide group but the lack of selectivity of these hCA inhibitors or related motifs is a pressing concern. In addition, Sulfanomide-containing medicines can also cause sulfa allergy, including life threatening anaphylaxis and Stevens-Johnson syndrome therefore the discovery of novel non-classical inhibitors of hCA targeting CA IX is the need of time [15–19].

Different pharmacological approaches have been utilized, such as the recognition of novel therapeutic targets, various structural related changes to the present compounds, the incorporation of two pharmacophores in a sole agent, and the utilization of structural variations, for example, spacers or linkers [20,21]. Enhancing evidence of the molecular complications of cancers and the developing resistance to anti-tumor therapy along with additional considerable clinical data, reveal that it is inconceivable to attain advantageous chemotherapeutic results regarding therapy of advanced stage cancers utilizing monotherapy. Multi-target strategy delivers not only substantial chemotherapeutic outcomes and ameliorates well-being but also lessens the likelihood of increasing drug resistance [22]. Poly-therapy may be accomplished by the combination of multiple drug cocktails, heterogeneous formations, or multi-target drugs [23].

The heterocyclic amines and their acetamide by-products have been recognized for their chemotherapeutic potential [24,25] which have been shown to exhibit several biological activities [23–26]. Hence, heterocyclic amine morpholine was employed as parent compound and a series of novel analogs was synthesized and characterized using spectral analysis [26,27]. The newly designed derivatives were further assessed for their inhibition mechanism of carbonic anhydrase along with their effect on ovarian cancer cell line and Hypoxia-inducible factor-1. Furthermore, the *in silico* molecular docking analysis was carried out to analyze the binding affinities together with patterns of bonding of these derivatives to which they interact with their target proteins. Our study for the first time reported the HIF-α activity of morpholine based derivatives.

2. Methodology

Melting points (m.p) were found out, utilizing a Gallen hamp [SANYO] model MPD BM 3.5 digital gadget. The spectral widths of Proton and C-13 NMR were estimated on a (Bruker) AM300 photometer in dimethyl sulfoxide at 300 MHz and 100 MHz using tetra methyl silane as an internal standard, respectively. FTIR study was performed with the help of Thermo Scientific (NICOLET IS10) spectrophotometer (ν max in cm-1) and (PerkinElmer) with an ANALYST 2000CHNS investigator was availed for assessment of existing molecules.

2.1. Preparation of 2-chloro-1-(morpholin-4-yl) ethanone (A)

Solution of morpholine (0.05 moL), in anhydrous dichloromethane (30 mL) was prepared, triethyl amine (or potassium carbonate) as a base was added to this solution, and 4.3 mL (0.05 moL) of chloroacetyl chloride was incorporated in dropwise manner meanwhile having the reaction mixture in ice bath for 15 min maintaining temperature between 0 and 5 °C. The chemical reaction was then mixed for 6 h at room temperature and the progression of the mixture was observed by Thin Layer Chromatography (Ethyl acetate: pet. Ether,

Table 1
The substituted R group used in the synthesis of morphline derivatives.

R = Groups (a-o)				
a) 	b) 	c) 	d) 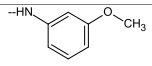	e) 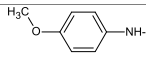
f) 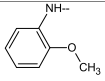	g) 	h) 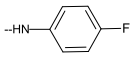	i) 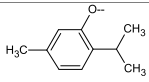	j) 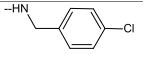
k) 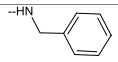	l) 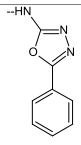	m) 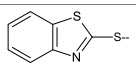	n) 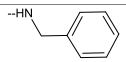	

3:1). After leaving the mixture at ordinary temperature for 24 h, it was flooded onto ice cubes. The solute separated by removing solvent to aridity under mitigated pressure using rotary evaporator. The dried solute (A) was recrystallized from ethanol (Ashraf et al., 2016). **(A)** 2-chloro-1-(morpholine-4-yl) ethanone; pale solid, yield (90 %); m. p. 122 °C; Retention factor 0.81 (ethyl acetate and petroleum ether, 3:1 v/v); mol. Wt; 163.6; molecular formula; C_6H_{10} $ClNO_2$.

2.2. Preparation of morpholine acetamide derivatives (1a-n)

In the solution of compound (A**)** of equimolar (0.05 moL), triethyl amine and anhydrous potassium iodide in N, N - dimethyl formamide (DMF) 25 mL was agitated at ordinary temperature pursued by adding 0.05moL of respective heterocyclic amine, phenol or thiol solution dropwise. At ambient temperature the mixture was agitated for 12 h. By using Thin Layer Chromatography, reaction progression was measured (Ethyl acetate: pet. Ether, 3:2). The mixture was purified with ethyl acetate and water several time, after extraction the compound was recovered from ethyl acetate on slow evaporation at standard ambient temperature. The isolated compound was cleansed with water, desiccated and crystallized again with ethanol [28]. In this way a series of acetamides were synthesized shown in Table 1.

2.3. Synthesis of 1,2-di (morpholin-4-yl) ethanone (1a)

Milky appearance solid, percentage yield (85 %), melting point 180 °C; Retention factor 0.76 (ethyl acetate and petroleum ether, 3:2 v/v); mol. Wt; 214.26; molecular formula; $C_{10}H_{18}N_2O_3$; CHN data % age calculated (obtained) Carbon, 56.06 (55.05); Nitrogen, 13.07 (12.06); Hydrogen, 8.47 (8.40); Oxygen, 22.40 (21.39). FT-IR ν (cm^{-1}): 2981 (CH), 1627 (CO, amide), 1258 (*C*–N). Proton NMR (^{1}H NMR) [(300 Megahertz, Dimethyl sulfoxide (DMSO), δ parts per million (ppm)]: 2.73 (s, 2H, –CH_2), 3.12–3.55 (m, 8H, Morpholine-H), 3.56–3.65 (m, 4H, Morpholine-H), 3.76–3.92 (m, 4H, Morpholine-H). Carbon-13 Nuclear Magnetic Resonance (100 MHz Dimethyl sulfoxide (DMSO-d_6) δ ppm): 49.8 (-CH_2), 54.7, 58.4, 63.3, Morpholine-C [65.3 (2Carbon, s), 63.3 (2Carbon, s), 54.7 (2Carbon, s), 58.4 (2Carbon, s)], 161.3 (C═O).

2.4. Synthesis of 1-(morpholin-4-yl)-2-(pyrrolidin-1-yl) ethanone (1 b)

Solid with dark brown appearance; percentage yield (80 %), melting point 170 °C; Retention factor 0.80 (ethyl acetate and petroleum ether, 3:2 v/v); mol. Wt; 198.26; molecular formula; $C_{10}H_{18}O_2N_2$; CHN data % age calculated (obtained) Carbon, 60.58 (59.58); Nitrogen, 14.13 (13.13); Hydrogen, 9.15 (9.01); Oxygen, 16.14 (15.13). FT-IR ν (cm^{-1}): 2977 (CH), 1635 (CO, amide), 1250 (*C*–N). Proton NMR (H NMR) (300 Megahertz, DMSO, δ parts per milion): 1.90 (m, 4H, Pyrrolidine-H), 2.57 (m, 4H, Pyrrolidine-H), 3.03 (s, 2H, –CH_2), 3.36–3.67 (m, 8H, Morpholine-H). C-13 NMR Spectroscopy (100 MHz Dimethyl sulfoxide (DMSO-d_6) δ parts per million): 49.8 (-CH_2), Pyrrolidine-C [24.6 (2Carbon, s), 44.5 (2Carbon, s)], Morpholine-C [66.5 (2Carbon, s), 53.4 (2Carbon, s)] 163.5 (C═O).

2.5. Synthesis of 1-(morpholin-4-yl)-2-(pyridin-2-ylamino) ethanone (1c)

Brown solid with crystalline appearance; percentage yield (78 %), melting point 178 °C; Rf 0.87 (ethyl acetate and petroleum ether, 3:2 v/v); mol. Wt; 221.2; molecular formula; $C_{11}H_{15}O_2N_3$; CHN data % age calculated (obtained) C, 59.71 (58.71); N, 18.99 (17.98); H, 6.83 (6.73); O, 14.46 (13.40). FT-IR ν (cm^{-1}): 3417 (NH), 2917 (CH), 1625 (CO, amide), 1446 (C═N), 1512 (C═C), 1265 (*C*–N). Proton NMR Spectroscopy (300 MHz, DMSO, δ parts per million): 2.90 (s, 2H, –CH_2), 3.38–3.46 (m, 4H, Morpholine-H), 3.54–3.57 (m, 4H, Morpholine-H), 6.39 (dd, 1H, $J = 6.7$, 6.8 Hz, Pyridyl-H), 6.44 (d, 1H, $J = 6.0$ Hz, Pyridyl-H), 7.54 (dd, 1H, $J = 6.9$, 6.4 Hz, Pyridyl-H), 8.25 (d, 1H, $J = 6.1$ Hz, Pyridyl-H), 9.11 (s, 1H, *N*–H). ^{13}Carbon NMR Spectroscopy (100 MHz Dimethy sulfoxide-d_6, δ parts per million): 49.8 (-CH_2), Morpholine-C [42.2 (2C, s), 62.4 (2C, s)], Pyridyl –C [127.7, 128.5, 137.5.148.1, 158.6)], 171.0 (C═O).

2.6. Synthesis of 2- [(3-methoxy phenyl) amino]-1-(morpholin-4-yl) ethanone (1 d)

Solid with yellowish brown appearance; yield (86 %), melting point 167 °C; Rf 0.75 (ethyl acetate and petroleum ether, 3:2 v/v); mol. Wt; 250.3; molecular formula; $C_{13}H_{18}N_2O_3$; CHN data % age calculated (obtained) C, 62.38 (61.29); N, 11.19 (10.19); H, 7.25 (6.15); O, 19.18 (19.0). FT-IR ν (cm^{-1}): 3360 (NH), 2947 (CH), 1695 (CO, amide), 1480 (C═C), 1293 (*C*–N), 1152 (*C*–O), 1033 (*C*–O). Proton NMR (300 MHz, DMSO, δ parts per million): 2.50 (s, 2H, –CH_2), 2.83 (s, 3H, OCH_3), 3.30–3.63 (m, 4H, Morpholine-H), 3.64–3.70 (m, 4H, Morpholine-H), 6.52 (d, 1H, $J = 6.2$ Hz, Ar–H), 6.76 (d, 1H, $J = 6.6$ Hz, Ar–H), 6.82 (d, 1H, $J = 6.2$ Hz, Ar–H), 7.10 (d, 1H, $J = 6.1$ Hz, Ar–H), 9.17 (s, 1H, *N*–H). C-13 NMR (100 MHz Dimethyl sulfoxide-d_6, δ parts per million): 49.7 (-CH_2), 65.5 (OCH_3) Morpholine-C [43.2 (2C, s), 64.8 (2C, s)], Ar–C [122.8, 123.4, 126.2, 131.2, 135.6, 143.8, 150.4)], 171.0 (C═O).

2.7. Synthesis of 2-[(4-methoxy phenyl) amino]-1-(morpholin-4-yl)ethanone (1e)

Blackish brown compound with solid appearance, melting point 185 °C; percentage yield (77 %); Retention factor 0.71 (ethyl acetate and petroleum ether, 3:2 v/v); mol. Wt; 250.3; molecular formula; $C_{13}H_{18}N_2O_3$; CHN data % age calculated (obtained) C, 62.38 (61.29); N, 11.19 (10.19); H, 7.25 (6.15); O, 19.18 (19.0). FT-IR ν (cm^{-1}): 3417 (NH), 2914 (CH), 1629 (CO, amide), 1504 (C═C), 1229 (*C*–N), 1111 (*C*–O), 1025 (*C*–O). Proton NMR Spectroscopy (300 MHz, Dimethly sulfoxide, δ parts per million): 2.54 (s, 2H,

–CH_2), 2.73 (s, 3H, OCH_3), 3.30–3.65 (m, 4H, Morpholine-H), 3.65–3.68 (m, 4H, Morpholine-H), 6.82–6,96 (m, 4H, Ar–H), 8.97 (s, 1H, *N*–H). Carbon-13 NMR Spectroscopy (100 MHz Dimethly sulfoxide-d_6, δ parts per million): 49.7 (-CH_2), 68.5 (OCH_3) Morpholine-C [44.2 (2Carbon, s), 66.4 (2Carbon, s)], Ar–C [120.4(2Carbon, s), 124.3(2Carbon, s), 148.3(2Carbon, s)], 161.4 (C═O).

2.8. Synthesis of 2-[(2-methoxyphenyl) amino]-1-(morpholin-4-yl) ethanone (1f)

Yellow solid with crystalline appearance, percentage yield (70 %); melting point 177 °C; Retention factor 0.63 (ethyl acetate and petroleum ether, 3:2 v/v); mol. Wt; mol. Wt; 250.3; molecular formula; $C_{13}H_{18}N_2O_3$; CHN data % age calculated (obtained) C, 62.38 (61.29); N, 11.19 (10.19); H, 7.25 (6.15); O, 19.18 (19.0). FT-IR ν (cm^{-1}): 3375 (NH), 2980 (CH), 1639 (CO, amide), 1450 (C═C), 1251 (*C*–N), 1107 (*C*–O), 1029 (*C*–O). Proton NMR Spectroscopy (300 MHz, DMSO, δ ppm): 2.57 (s, 2H, –CH_2), 2.90 (s, 3H, OCH_3), 3.30–3.66 (m, 4H, Morpholine-H), 3.60–3.68 (m, 4H, Morpholine-H), 6.80–6.98 (m, 4H, Ar–H), 8.76 (s, 1H, *N*–H). Carbon-13 NMR Spectroscopy (100 MHz Dimethly sulfoxide-d_6, δ parts per million): 49.3(-CH_2), 67.5 (OCH_3) Morpholine-C [41.2 (2C, s), 59.8 (2C, s)], Ar–C [121.2, 122.2, 123.5, 131.2, 134.6, 145.4, 150.8], 170.0(C═O).

2.9. Synthesis of 1-(morpholin-4-yl)-2-phenoxyethanone (1 g)

Brown solid of crystalline appearance, percentage yield (78 %); melting point 200 °C; Retention factor 0.88 (ethyl acetate and petroleum ether, 3:2 v/v); mol. Wt; 221; molecular formula; $C_{12}H_{15}NO_3$; CHN data % age calculated (obtained) C, 65.14 (64.29); N, 6.33 (5.19); H, 6.83 (6.25); O, 21.69 (21.0). FT-IR ν (cm^{-1}): 2855 (CH), 1632 (CO, amide), 1449 (C═C), 1255 (*C*–N) Proton NMR (300 Megahertz, Dimethyl sulfoxide, δ parts per million): 2.80 (s, 2H, –CH_2), 3.36–3.62 (m, 4H, Morpholine-H), 3.64–3.66 (m, 4H, Morpholine-H), 6.82–7.12 (m, 4H, Ar–H), 9.40 (s, 1H, *N*–H). Carbon NMR (100 MHz Dimethly sulfoxide-d_6, δ parts per million): 49.7 (-CH_2), Morpholine-C [41.2 (2Carbon, s), 66.8 (2Carbon, s)], Ar–C [120.8, 127.4, 130.4, 134.6, 147.2, 157.2)], 171.7 (C═O).

2.10. Synthesis of 2-[(4-fluorophenyl) amino]-1-(morpholin-4-yl) ethanone (1 h)

Dark yellow crystalline solid, mp 220 °C; yield (71 %); Rf 0.83 (ethyl acetate and pet. Ether, 3:2 v/v); mol. Wt; 238; molecular formula; $C_{12}H_{15}FN_2O_2$; CHN data % age calculated (obtained) C, 60.49 (60.42); N, 11.76 (11.66); H, 6.35 (6.31); O, 13.43 (13.03). FT-IR ν (cm^{-1}): 3145 (NH), 2998(CH), 1633(CO, amide), 1503 (C═C), 1221(*C*–N), 816 (*C*–F). ^{1}H NMR (300 MHz, DMSO, δ ppm): 3.52–3.68 (m, 4H, Morpholine-H), 3.67–3.69 (m, 4H, Morpholine-H), 3.99 (s, 2H, –CH_2), 6.91 (d, 2H, $J = 6.2$ Hz, Ar–H), 7.16 (d, 2H, $J = 6.4$ Hz, Ar–H), 9.23 (s, 1H, *N*–H). ^{13}C NMR (100 MHz DMSO-d_6, δ ppm): 49.5 (-CH_2), Morpholine-C [58.7 (2C, s), 46.5 (2C, s)], Ar–C [123.4, 120.2135.6.140.4, 146.2, 158.1)], 173.4 (C═O).

2.11. Synthesis of 2-[5-methyl-2-(propan-2-yl) phenoxy]-1-(morpholin-4-yl) ethanone (1i)

Crystalline solid of red colour, percentage yield (76 %); melting point 172 °C; Retention factor 0.64 (ethyl acetate and petroleum ether, 3:2 v/v); mol. Wt; 277; molecular formula; $C_{16}H_{23}NO_3$; CHN data % age calculated (obtained) C, 69.29 (68.27); N, 5.05 (4.99); H, 8.36 (8.06); O, 17.31 (17.01). FT-IR ν (cm^{-1}): 2958 (CH), 1625 (CO, amide), 1513 (C═C), 1227 (*C*–N), 1157 (*C*–O), 1090 (*C*–O). Proton NMR (300 Megahertz, Dimethyl sulfoxide, δ parts per million): 1.29 (m, 6H, Aliphatic-H), 2.12 (s, 3H, CH_3), 2.40 (s, 2H, –CH_2), 2.95–3.01 (m, 1H, Ar–H), 3.56–3.65 (m, 8H, Morpholine-H), 6.80–7.26 (m, 3H, Ar–H). Carbon-13 NMR (100Megahertz Dimethyl sulfoxide-d_6, δ parts per million): 49.2 (-CH_2), Morpholine-C [45.2 (2Carbon, s), 65.8 (2Carbon, s)], Ar–C [122.8, 123.4, 126.2, 130.6, 135.2, 140.4, 148.4, 153.8, 156.3, 160.1], 175.0 (C═O).

2.12. Synthesis of 2-[(4-chlorobenzyl) amino]-1-(morpholin-4-yl) ethanone (1j)

Pale yellow solid of crystalline appearance, percentage yield (87 %); melting point 190 °C; Retention factor 0.89 (ethyl acetate and petroleum ether, 3:2 v/v); mol. Wt; 268; molecular formula; $C_{13}H_{17}ClN_2O_2$; CHN data % age calculated (obtained) C, 58.10 (57.30); N, 10.42 (12.06); H, 6.38 (6.08); O, 11.91 (10.27). FT-IR ν (cm^{-1}): 3304 (NH), 2970 (CH), 1679 (CO, amide), 1591 (C═C) 1235 (*C*–N), 880 (*C*–Cl). Proton NMR (300 Megahertz, DMSO, δ parts per million): 3.52–3.60 (m, 4H, Morpholine-H), 3.61–3.63 (m, 4H, Morpholine-H), 3.75 (s, 2H, –CH_2), 3.90 (s, 2H, –CH_2), 7.35–7.46 (m, 4H, Ar–H), 9.10 (s, 1H, *N*–H). Carbon-13 NMR (100Megahertz Dimethyl sulfoxide-d_6, δ parts per million): 43.2 (-CH_2), 45.2 (-CH_2), Morpholine-C [45.2 (2C, s), 65.8 (2C, s)], Ar–C [125.2, 128.4, 135.6, 153.8, 160.1, 173.3], 175.0 (C═O).

2.13. Synthesis of 2-[(4-fluoro benzyl) amino]-1-(morpholin-4-yl) ethanone (1 k)

White solid with crystalline appearance, percentage yield (79 %); melting point 185 °C; Retention factor 0.78 (ethyl acetate and petroleum ether, 3:2 v/v); mol. Wt; 252; molecular formula; $C_{13}H_{17}FN_2O_2$; CHN data % age calculated (obtained) C, 61.89 (60.09); N, 11.10 (10.10); H, 6.79 (6.09); O, 12.68 (12.08). FT-IR ν (cm^{-1}): 3204 (NH), 2902 (CH), 1679 (CO, amide), 1513 (C═C), 1253 (*C*–N), 1131(*C*–O), 880 (*C*–F). Proton NMR (300 MHz, DMSO, δ ppm): 2.40 (s, 2H, –CH_2), 3.70 (s, 2H, –CH_2), 3.56–3.62 (m, 4H, Morpholine-H), 3.63–3.69 (m, 4H, Morpholine-H), 7.01–7.16 (m, 4H, Ar–H), 9.20 (s, 1H, *N*–H). Carbon-13 NMR (100 Megahertz, Dimethyl sulfoxide-d_6, δ parts per million): 44.2 (-CH_2), 47.2 (-CH_2), Morpholine-C [43.2 (2C, s), 61.8 (2C, s)], Ar–C [124.2, 129.4, 137.6, 150.1, 154.8, 165.3], 175.0 (C═O).

2.14. Synthesis of 1-(morpholin-4-yl)-2-[(5-phenyl-1,3,4-oxadiazol-2-yl) amino] ethanone (1 l)

White-coloured solid with powder appearance, percentage yield (91 %); melting point 162 °C; Retention factor 0.61 (ethyl acetate and petroleum ether, 3:2 v/v); mol. Wt; 288; molecular formula; $C_{14}H_{16}N_4O_3$; CHN data % age calculated (obtained) C, 58.32 (58.0); N, 19.43 (19.02); H, 5.59 (5.09); O, 16.65 (16.08). FT-IR ν (cm^{-1}): 3328 (NH), 2930 (CH), 1667 (CO, amide), 1627 (C═N), 1521 (C═C). Proton NMR (300 Megahertz, DMSO, δ parts per million): 2.92 (s, 2H, $–CH_2$), 3.56–3.69 (m, 8H, Morpholine-H), 7.10–7.96 (m, 5H, Ar–H), 9.40 (s, 1H, *N*–H). Carbon-13 NMR (100 Megahertz, Dimethyl sulfoxide-d_6, δ parts per million): 49.2 ($-CH_2$), Morpholine-C [66.4 (2C, s), 65.3 (2C, s)], Ar–C [120.2, 123.2, 125.8, 128.4, 133.4, 139.6.142.4150.8], 172.0 (C═O).

2.15. Synthesis of 2-(1,3-benzothiazol-2-ylsulfanyl)-1-(morpholin-4-yl) ethanone (1 m)

White solid of crystalline appearance, percentage yield (89 %); melting point 206 °C; Retention factor 0.59 (ethyl acetate and petroleum ether, 3:2 v/v); mol. Wt; 294; molecular formula; $C_{13}H_{14}N_2O_2S_2$; CHN data % age calculated (obtained) C, 53.04 (52.0); N, 9.52 (9.45); H, 4.79 (4.74); O, 10.87 (10.77). FT-IR ν (cm^{-1}): 3248 (NH), 2902 (CH), 1676 (CO, amide), 1612 (C═N), 1497 (C═C), 902 (*C*–S). Proton NMR (300 MHz, DMSO, δ ppm): 3.12 (s, 2H, $–CH_2$), 3.57–3.69 (m, 8H, Morpholine-H), 7.10–7.76 (m, 2H, Ar–H), 7.76–7.96 (m, 2H, Ar–H). Carbon-13 NMR (100 MHz, Dimethyl sulfoxide-d_6, δ parts per million): 49.1 ($-CH_2$), Morpholine-C [53.7 (2C, s), 44.5 (2C, s)], Ar–C [123.4, 126.2, 130.2, 135.6140.4, 148.4, 160.1], 174.4 (C═O).

2.16. Synthesis of 2-(benzyl amino)-1-(morpholin-4-yl) ethanone (1n)

White solid with amorphous appearance, percentage yield (74 %); melting point 240 °C; Retention factor 0.86 (ethyl acetate and petroleum ether, 3:2 v/v); mol. Wt; 234; molecular formula; $C_{14}H_{16}N_4O_3$; CHN data % age calculated (obtained) C, 66.64 (66.14); N, 11.96 (11.06); H, 7.74 (7.24); O, 13.66 (13.43). FT-IR ν (cm^{-1}): 3345 (NH), 2950 (CH), 1637 (CO, amide), 1511 (C═C) 1254 (*C*–N), 1001 (*C*–O). Proton NMR (300 Megahertz, DMSO, δ parts per million): 2.50 (s, 2H, $–CH_2$), 3.54–3.57 (m, 4H, Morpholine-H), 3.61–3.63 (m, 4H, Morpholine-H), 3.67 (s, 2H, $–CH_2$), 7.05–7.46 (m, 5H, Ar–H), 9.05 (s, 1H, *N*–H). Carbon-13 NMR (100 MHz Dimethyl sulfoxide-d_6, δ ppm): 48.8 ($-CH_2$), 47.6 ($-CH_2$), Morpholine-C [65.3 (2C, s), 44.5 (2C, s)], Ar–C [123.4, 126.2, 135.6, 140.4, 148.2, 160.1], 174.3 (C═O).

2.17. In vitro assay for inhibition of carbonic anhydrase (CA-IX)

In vitro assay of carbonic anhydrase inhibition was conducted by the reported method [29]. The principle is to spectrophotometrically quantified p-nitro phenol, the esterase activity of active carbonic anhydrase (CA) on an ester substrate of p-nitro phenyl acetate. After standardization of chemicals and method, 50 mM Tris-sulfate buffer (*pH* 7.6, having 0.1 mM $ZnCl_2$) 60 μL, test compound in 1 % Dimethyl sulfoxide (DMSO) 10 μL (0.5 mM), and bovine enzyme 10 μL (50 U) were taken as reaction mixture in each well. The components were amalgamated and incubated at 25 °C for 10 min 96-well plate reader was used to read the plates at 348 nm. Substrate, 20 μL *p*-nitrophenyl acetate was freshly prepared (6 mM stock using <5 % acetonitrile in buffer), and transferred to each well to attain the concentration of 0.6 mM per well. The total volume of the reaction mixture was made up to 100 μL, and incubate for 30 min at 25 °C. After incubation, the ingredients were mixed together and read at 348 nm. In CA inhibition assay, appropriate controls with dimethyl sulfoxide (DMSO) and standard inhibitor acetazolamide (AZM) were also included. Mean of three independent experiments (±SEM) were calculted and results were reported. The results were expressed as percent inhibitions calculated by the formula given below:

$$(\%)\ \text{Inhibition} = [1\text{-}(A / B)]x100$$

Where; A denoted absorbance value for experimental wells.
B denoted control wells.

2.18. MTT assay

The cytotoxic activity of compounds was assessed through the MTT assay using hypoxia induced ID8 mouse ovarian epithelial cell line (ATCC® SCC145). The cells were implanted into sterile 96-well cell culture plates and, treated with test compounds and control. At 72 h post drug addition, 3-(4,5-dimethylthiazol-2-yl)-2,5-diphenyltetrazolium bromide (MTT) was added to the 96-well plates, and re-suspended crystals of formazan were analyzed. The cell growth inhibition percentage (%) was represented as [1-(A/B)] *100, where A was absorbance value for experimental wells and B for control wells. The IC50 values were measured using Graph Pad Prism-6 [30]; [31].

2.19. Quantitative HIF-1α inhibitory assay

To evaluate the activity of Hypoxia-inducible factor 1-alpha (HIF-1α), ab275103 mouse HIF-1α simple step ELISA Kit was employed according to the manufacturer's instructions (Abcam China). First, the concentrates of cell lysate prepared from the fresh materials were shifted into 96-well plate with immobilized double-stranded DNA sequences having the HIF-1α binding HREs. HIF-1α binding

was assessed using a primary mouse *anti*–HIF–1α antibody and a secondary labeled anti-mouse antibody. Absorbance (OD) was estimated through spectrophotometer at 450 nm [32].

2.20. Pharmacokinetic parameters

The PK properties adsorption, distribution, metabolism, excretion, and toxicity (ADMET) of test compounds and drug-like nature were investigated. As per Lipinski rule-5, drug-like molecules should have ≤5 H-bond donors, ≤10 H-bond acceptors, Molecular Weight <500 Da, and Partition coefficient (logP) ≤5. All the compounds synthesized were checked for their drug likeliness in relevance with anticancer properties confirmed *via* aid of online server Molinspiration Cheminformatics (Table 4) and SAR-studies.

2.21. Molecular docking studies

2.21.1. Selection of ligand and optimization

Docking study was done in order to determine the structures of newly synthesized compounds **(1a)** to **(1n)** using Discovery Studio Visualizer 2017, saved as PDB format and further adapted to pdbqt format using Autodock Tools 1.5.6. Gasteiger charges applied to all atoms by the Auto Dock Tools, moreover it also added polar hydrogens and eliminated non-polar hydrogens from all the ligands.

2.21.2. Accession of target protein

The structures of Human carbonic anhydrase IX (PDB ID: 6VKG) and hypoxia inducible factor-1 (PDB ID: 1L3E) were selected for screening of ligands [33]. The molecules of water and co-crystallized ligands were separated from protein structures and they were transformed to pdbqt format by AutoDock Tools 1.5.6. The Zinc ion present in 6VKG was not eliminated as it can result in formation of electrovalent bonding between target proteins and ligands.

2.21.3. Target protein optimization

The binding site was described on the bases of co-crystallized Ligands existing in protein structures and search space was restricted to get binding poses of ligands as much identical in orientation as possible to co-crystallized ligands. AutoDock Vina was used for obtaining the docked poses along with score. The docking of co-crystallized ligands were also conducted as reference for comparison and verification of the results.

2.21.4. Assessment of active binding sites

The binding site was described and investigated on the bases of co-crystallized ligands present in protein structures and search space was controlled to obtain poses of ligands as much alike in configuration as possible to co-crystallized ligands to authenticate the docking protocols. The grid was set at Center X:11.530, Y: 1.4135, Z: 16.047 and the Dimensions (Angstrom) X: 46.64, Y: 43.82 and Z: 54.45. The grid size for IL3e was set at center X: 30.99, Y: 51.30, Z: 46.83 and the dimension (Angstrom) X: 41.30, Y: 48.95 and Z: 46.83. The docked poses of ligands as well as score were reported by using Auto Dock Vina. The best scoring poses were rescored with the help of x-score. The docking of co-crystallized ligands were also conducted as reference for comparison and verification of the results. The binding energies of best ligand poses was acquired by Auto Dock Vina in Kcal/mol and their rescoring estimations by X-Score in PKd.

2.21.5. Confirmation of docking

The procedure of docking was validated by again docking the acquired pose on the same active binding site of target protein. All the protocols were remained constant keeping the grid parameters unchanged. If the ligand binds to the binding site with less deviation in

Table 2
IC_{50} values for compounds **1a-1n** (CA-IX inhibition data).

Compound	IC_{50}± SEM (μM) (CA-IX)
1a	12.52 ± 0.51
1b	11.36 ± 0.77
1c	8.80 ± 0.56
1d	11.13 ± 0.13
1e	33.85 ± 1.97
1f	30.45 ± 0.81
1g	10.31 ± 0.40
1h	8.12 ± 1.50
1i	17.00 ± 0.58
1j	12.31 ± 0.77
1k	25.50 ± 0.65
1l	22.13 ± 0.17
1m	12.80 ± 1.22
1n	22.44 ± 0.41
Acetazolamide	7.51 ± 2.60

Table 3
The effects of compounds (**1a-1n**) on the viability of Ovarian cancer cell lines ID8 (n = 3). IC_{50} values of synthesized compounds and reference drug cisplatin.

	Compound	IC_{50} (μM)
1.	**1a**	23.86 ± 0.61
2.	**1b**	14.8 ± 0.70
3.	**1c**	15.68 ± 0.64
4.	**1d**	25.27 ± 0.82
5.	**1e**	26.45 ± 0.72
6.	**1f**	158.4 ± 0.66
7.	**1g**	146.1 ± 0.56
8.	**1h**	**9.407 ± 0.73**
9.	**1i**	**11.2 ± 0.22**
10.	**1j**	21.49 ± 0.11
11.	**1k**	64.17 ± 0.88
12.	**1l**	15.64 ± 0.77
13.	**1m**	32.39 ± 0.67
14.	**1n**	47.92 ± 0.75
15.	**Cisplatin**	**8.502 ± 0.23**

Table 4
Pharmacokinetic and ADMET parameters of synthesized compounds.

	miLogP	TPSA	natoms	MWt	HBA	HBD	nviolations	nrotb	volume
1a	1.45	64.64	33	214.26	5	1	0	6	210.11
1b	−1.13	93.45	32	198.26	6	4	0	4	190.45
1c	2.51	79.79	31	221.2	6	2	0	7	211.25
1d	2.23	100.02	36	250.3	7	3	0	6	211.85
1e	4.24	93.46	36	250.3	7	2	0	6	238.21
1f	4.61	76.47	36	250.3	7	1	0	1	208.1
1g	4.51	73.23	31	221.0	6	1	0	6	222.2
1h	0.83	64.36	32	238.0	4	3	0	3	219.5
1i	0.83	64.36	43	277.0	4	3	0	3	266.5
1j	4.05	50.36	35	268.0	4	2	0	6	256.44
1k	4.19	70.92	35	252.0	5	2	0	5	247.89
1l	6.21	64.36	37	288.0	5	1	1	5	276.26
1m	6.58	47.37	33	294.0	5	0	1	6	241.15
1n	6.47	44.13	37	234.0	4	0	1	5	228.24

miLogP* = Molinspiration logP value, TPSA* = total polar surface area, MWt* = molecular weight, HBA* = hydrogen bond acceptor, HBD* = hydrogen bond donor, n violations* = number of Rule of 5 violations, and nrotb* = number of rotatable bonds.

comparison to the actual complex, the validation of molecular docking is confirmed. By using Discovery studio 4.0 and PyMOL 203 the redocked complex was superimposed on the reference complex. The root mean square was calculated to analyze the deviation and the superimposed image was generated showing the amino acid residues.

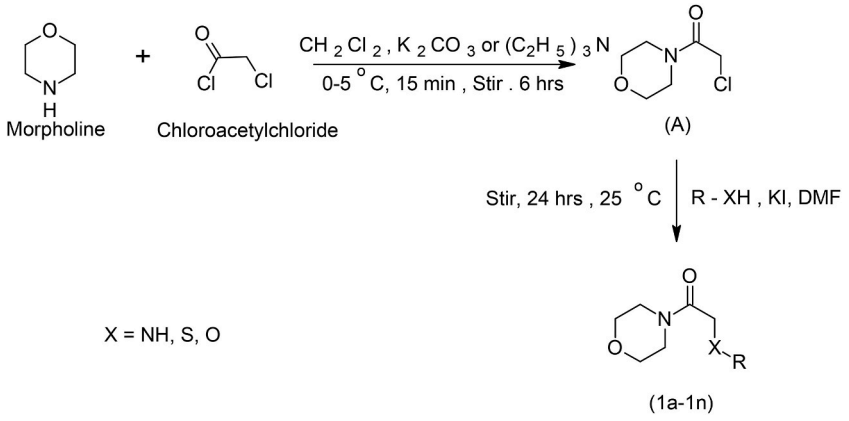

Fig. 1. Scheme of synthesis of morpholine derivatives.

3. Results

3.1. Chemistry

Scheme of synthesis for the formation of the test compounds has been shown in Fig. 1. The scheme comprised of reaction of morpholine with chloroacetyl chloride and the subsequent by-product chloroacetamide **(A)** was reacted with different alcohols, amines, and thiol to obtain heterocyclic amine derivatives (**1a-1n),** respectively. All the synthesized compounds exhibited excellent yield. Fourier transform infrared (FTIR), Proton nuclear magnetic resonance (^{1}H NMR), Carbon nuclear magnetic resonance (^{13}C NMR) and elemental analysis were employed for the characterization of synthesized compounds. Physical data including the melting points was also recorded. Solubility data showed that most of the compounds from (**1a-1n)** were soluble in dimethyl sulfoxide (DMSO), ethanol and ethanolic water but compound **1g, 1j** and **1n** were only soluble in DMSO.

3.2. In vitro carbonic anhydrases (CA-IX) inhibition assay

The synthesized compounds (**1a-1n**) were screened against carbonic anhydrase enzyme to analyze the inhibitory potential of synthesized compounds (Table 2). For comparison, clinically used inhibitor, acetazolamide was employed as a standard. A remarkable increase in carbonic anhydrase (CA) inhibition activities was detected in morpholine derivatives consisting the alcoholic and amine substituents. The most active derivatives were **1h** and **1c** having IC_{50} comparable to that of standard. The standard showed the lowest IC_{50} of 7.51 μM while, **1h** and **1c** showed similar pattern of inhibition having IC_{50} of 8.12 μM (μM) and 8.80 μM (μM), respectively. The compounds **1g** also showed reasonable inhibition having IC_{50} of 10.31 μM. The CA inhibition activity was in the order 1 h > 1c > 1 g > 1 d > 1 b > 1j > 1a >1 m > 1i > 1 l > 1n > 1 k > 1f > 1e.

3.3. MTT assay

In order to assess the anticancer potencies of produced compounds, MTT analysis was employed against hypoxia induced ovarian cancer cell line ID8. The outcomes depicted that the test molecules revealed considerable inhibitory activities when compared with control cisplatin. The compound **1h** and **1i** showed maximum inhibition at 50 μM concentration with IC_{50} of 9.47 and 11.2 μM, respectively. This was comparable to standard cisplatin having 60 % inhibition with IC_{50} 8.5 μM. The compounds **1b, 1c** and **1l** showed IC_{50} of 14.8, 15.68 and 15.64 μM at the same concentration. The compound **1l** also showed 60 % inhibition of cells at similar concentration. Table 3 and Fig. 2 show the percent inhibition of cellular proliferation at different concentrations.

3.4. Quantitative HIF-1α through ELISA

The results of HIF-1α assay have been graphically expressed in Fig. 3. All cell extracts exhibited a significant inhibition of HIF-1α as compared to saline. Control sample extract exhibited the maximum inhibition while inhibitory activity of **1b** sample extract was comparable to the control. In addition, the sample extracts **1c, 1h, 1i** shown optimal activity whereas, **1d** exhibited lesser inhibition of **HIF-1α** as compared to other molecules.

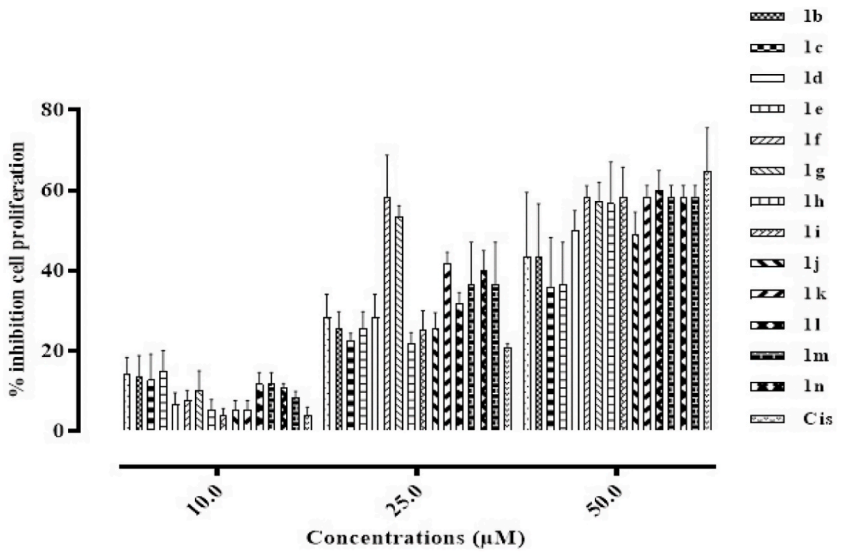

Fig. 2. The effects of synthesized compounds (**1a-1n**) on the % inhibition of cell proliferation in Ovarian cancer cell lines ID8 (n = 3) at different concentrations in synthesized compounds and control drug cisplatin.

3.5. Cheminformatics analysis

Table 3 presents pharmacokinetic parameters of newly synthesized compounds evaluated by molinspiration and cheminformatics online servers (https://www.molinspiration.com/). All the novel compounds manifested the Lipinski rule of 5 and were found to follow the minimum structural requirements for a candidate drug molecule.

3.6. Docking studies

The consequences of molecular docking analysis revealed that the synthesized compounds exhibited moderately high binding with carbonic anhydrase IX and HIF-1α. The compound **1i** showed optimum binding affinity with carbonic anhydrase CA-IX enzyme of −6.9 kcal/mol. The binding was comparable to that of standard epacadostat (inhibitor of enzyme CA-IX) having binding energy −7.2 kcal/mol. The compounds **1h** and **1d** also showed lowest binding energy of −6.7 and −6.5 kcal/mol, respectively. The binding interactions of active compounds with the target protein was analyzed to study the amino acids involved in interaction (Fig. 4) and co-crystal ligand was also used for studying the binding interaction in docking analysis which confirmed method validation as well [34]. The docking analysis exhibited that the compound **1b** formed strong hydrogen bond with ASN11, carbon hydrogen bond formation was also observed with GLY6 and pi-alkyl interactions with PHE231. The compound **1c** also showed conventional hydrogen bonding with HIS4, carbon hydrogen bond formation was observed with GLU170 and ASN62 and pi-*pi stacked interaction with PHE*231. The interaction analysis of compound **1d** showed a conventional hydrogen bonding with GLY8 and pi-*pi stacked interactions with PHE*231. A similar pattern of interaction was observed with **1h** but with three conventional hydrogen bonding between TYR7, GLY8, ASN11 and oxygen of acetamide. A pi-sigma bonding was also seen with PHE231. The binding analysis of compound 1i revealed conventional hydrogen bonding with ASN11, carbon hydrogen bond with ASN62 and HIS64 and a *pi sigma interaction with PHE*231. All the compounds manifested interaction within the active binding site.

The docking studies of the synthesized compounds with HIF-1α were also observed (Fig. 5). The analysis revealed conventional hydrogen bonding of compound **1b** with ARG165, carbon hydrogen (*C*–H) bond with ASN230 and CYS128, and an alkyl interactivity with LEU126. The compound **1c** showed some van der Waals interaction with GLY216, conventional hydrogen bonding with SER195, and a carbon hydrogen (*C*–H) bond with GLN192. Amide *pi stacked interconnections were also showed between phenyl ring and CYS*191, and TRP215. In compound **1h**, three firm conventional hydrogen bonding was displayed between oxygen atoms and GLY193 and SER195. A carbon hydrogen bond was also observed with SER214 in addition to an alkyl interaction with the VAL213. The binding interaction of compound **1i** also revealed a stable three conventional hydrogen bond with ARG76 and GLN80. Carbon hydrogen bond was observed with LEU73, a pi-pi stacked and pi-*pi T shaped interaction was also observed with TYR*34 and a pi-sigma interaction with PHE66.

Docking validation was also performed to make certain the docking strengths and to validate the procedure by redocking the leading pose in the active binding site of target protein. The redocking revealed the binding of ligand in the same active site having rmsd 0.1 kcal/mol. The amino acids participating in binding interactions were SER195, GLY193, SER214 and VAL213. The native co-crystallized ligand was superimposed in the docked complex using PyMOL. An extremely low rmsd of 0.1 indicated the confirmation of docking method (Fig. 6). The forest green complex represents the reference conformation achieved during docking while the red complex displays the redocked complex of **1h** in the active binding site of HIF-1α protein. Similarly, the blue complex marks the reference complex obtained during docking while the yellow complex signifies the redocked complex of epacadostat in the active binding site of carbonic anhydrase protein with rmsd of 0.5 kcal/mol.

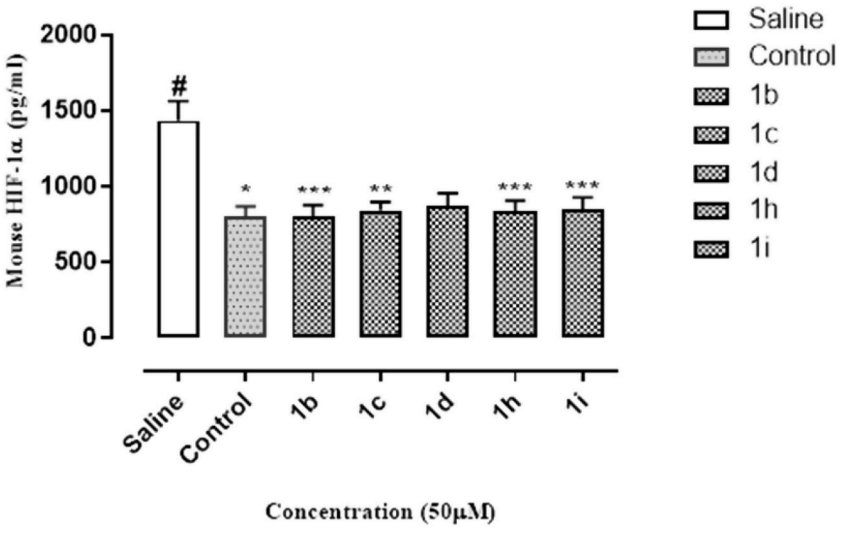

Fig. 3. Percent inhibition of HIF-1α by **1b, 1c, 1d, 1h** and **1i** at 50 μM concentration.

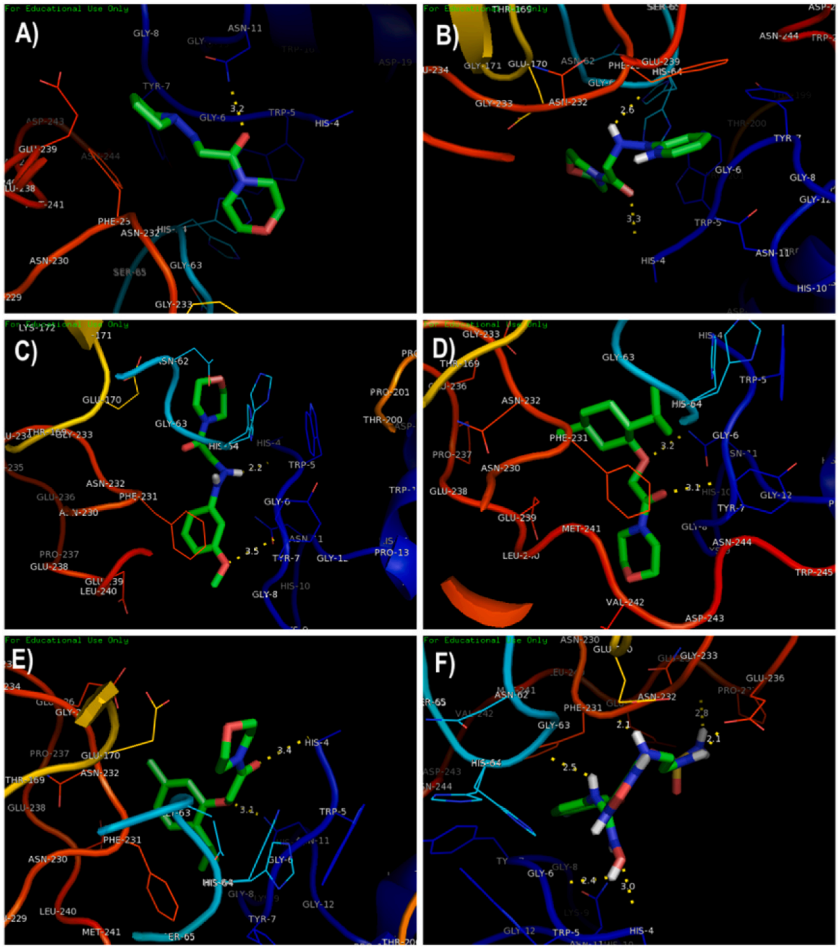

Fig. 4. Two-dimensional (2D) presentation of binding interactions of synthesized compounds with the amino acid residues at the active binding site of Carbonic Anhydrase IX (PDB ID: 6VKG). **(A)** Binding Interaction of ligand **1b (A), 1c (B), 1d (C), 1h (D), 1i (E),** and standard epacadostat **(F)** with carbonic anhydrase IX.

4. Discussion

Carbonic anhydrases are the zn-containing metalloenzymes responsible for catalyzing reversible interconversion of CO_2 and bicarbonate [35–37]. As a result of catalysis weak base bicarbonate ions and a strong acid, H^+ are produced after efficient hydration of CO_2 through hydroxide intermediate. The enzymes are associated with regulating pH, electrolyte metabolism, and secretion in healthy and cancerous cells. Overexpression of two isoenzymes CAIX and XII has been observed in hypoxic tumors in fifteen CA isoforms. As a consequence of activation of hypoxia inducible factor (HIF-1a) transcription factor the hypoxic tumors develop [38,39]. The factor has been shown to be expressed under hypoxic conditions and has crucial role in the biological adaptive feedback to hypoxia. The expression of HIF1α is also related to the activation of target gene expression including carbonic anhydrase IX [40–43]. The overexpression of CAIX has been observed in several malignant tumors and cancers having association with breast carcinomas, bladder cancer as well as lung cancer [44–46]. The data suggesting the overexpression of CA-IX in the occurrence of ovarian cancer has limited availability. However, various reported ovarian tumors showed wide expression of CAIX [47–49]. In another study, a tissue microarray analysis of tumor samples was surveyed for CAIX overexpression in ovarian cancer and the evidence suggested link of CAIX overexpression with poor outcome in ovarian patients. The study highlighted CAIX as potential therapeutic drug target in human cancer. Based on these evidences, varieties of novel morpholine compounds were synthesized and characterized. The compounds were studied for their carbonic anhydrase inhibitory potential and their role as HIF1α inhibitors. The effect of these compounds were also studied in ovarian cancer to analyze whether morpholine based compounds would be beneficial in targeting ovarian cancer.

The produced compounds were differentiated using spectral studies. IR spectrum confirmed the structure as carbon halogen bond showed absorption bands at (804–880) cm^{-1} whereas other common absorption peaks observed in all derivatives are (1111–1293) cm^{-1} for carbon-nitrogen bond, (1450–1591) cm^{-1} for C═C, for carbon double bond with nitrogen, (1001–1157) cm^{-1} for carbon-oxygen bond, (1595–1679) cm^{-1} for carbonyl groups of amide, (2912–3048) cm^{-1} for linker CH_2 bending which is characteristic peak of absorptions in all compounds respectively. H^1-NMR of synthesized compounds showed the peaks of all functionalities in their

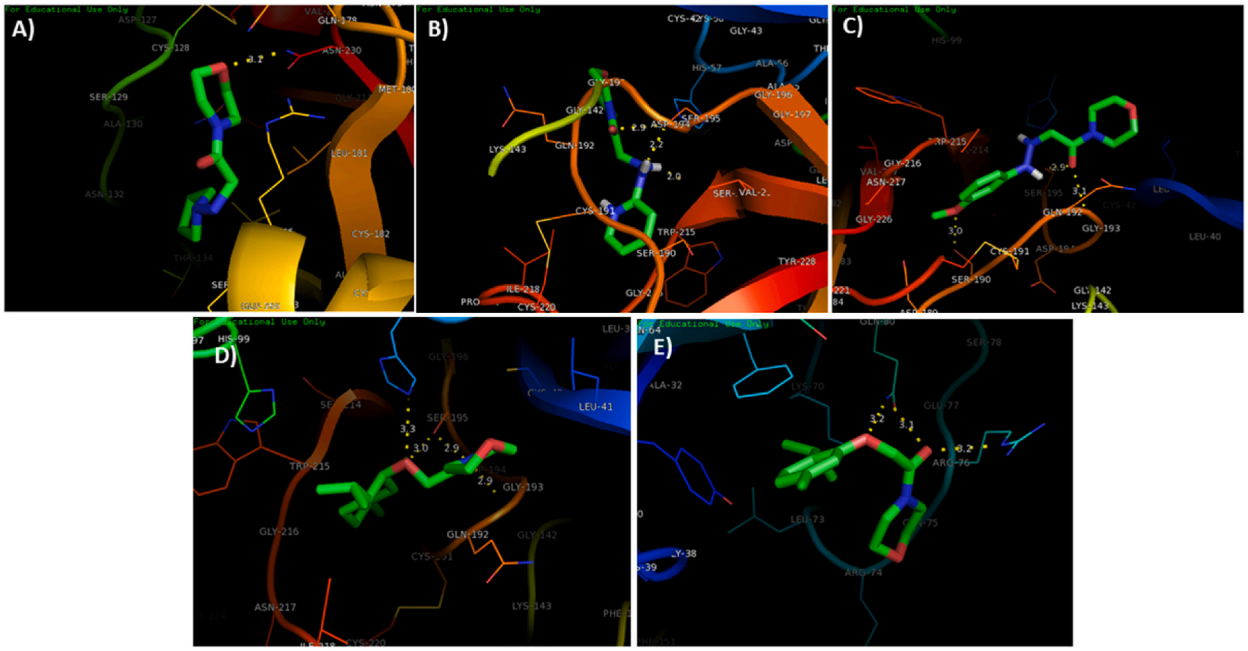

Fig. 5. Molecular docking analysis of active ligands **1b (A), 1c (B), 1d (c), 1h (D)** and **1i (E)** in the active binding site of target protein HIF-1α (PDB ID: 1L2E).

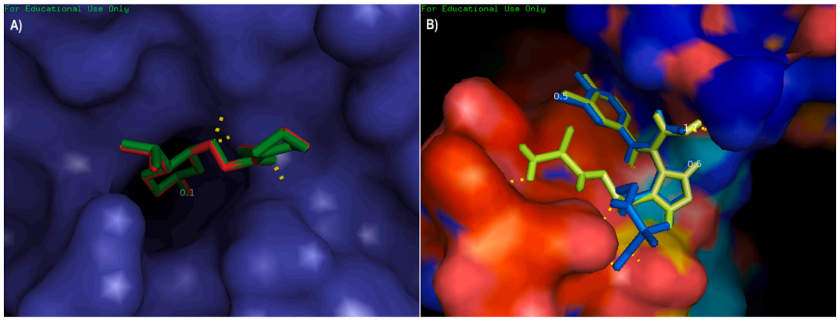

Fig. 6. Superimposition of re-docked complex with the reference complex**. (A)** The redocked complex is superimposed onto the reference conformation **1h** in the active binding site of 1L2E protein. **(B)** The re-docked complex is superimposed onto the reference conformation epacadostat in the active binding site of 6 KVG.

respective region, for instance, in the case of most active compound of **1h** characteristic peak of linker CH_2 observed at 3.91 ppm (2H, s), and present in all derivatives in the between 2.89 and 3.91 ppm proving their synthesis, while aromatic proton resonated at 6.08–7.87 ppm. Overexpression of hCA IX is evident of many physiological conditions like malignancies and hypoxic tumors therefore isozyme of hCA IX is a pharmaceutical target and biomarker for many cancers. Even though the characteristics of hCA inhibitors interactions with the enzyme's catalytic region are well understood but the lack of selectivity of classic hCA inhibitors based on the sulfonamide group or related motifs is a pressing concern. Sulfanomide-containing medicines can also cause sulfa allergy therefore identification of novel non-classical inhibitors of hCA targeting CA IX is a top priority that is now undergoing extensive research. Therefore, the formulated dervatives were studied for their enzymatic carbonic anhydrase activity against CA-IX isoenzyme. Most of the derivatives reported excellent out-turns possessing practicable carbonic anhydrase inhibitory activity specificallly compounds **1c, 1h** and **1g** exhibiting appropriate CA inhibition activity.

The lowest IC_{50} was shown by **1h** with 4-fluro aniline moiety of 8.12 μM which was equivalent to the standard acetazolamide with IC_{50} of 7.51 μM. The compound **1c** having amino pyridine moiety also showed significant IC_{50} of 8.80 μM at similar concentration and compound **1g** with phenoxy moiety showed IC_{50} 10.31 μM respectively. From our result it is evident that the compounds with heterocyclic moieties like in the case of compound **1c** and the compound with substituted aryl ring system, especially substitution of electronegative atom enhances activity as in compound **1h**, that are more active then compounds with unsubstituted simple aryl ring as in compound **1g** (Fig. 7).

A morpholine based novel series of 2-morpholino-4-phenylthiazol-5-yl acrylamide derivatives were synthesized by Swain and co-

workers, who analyzed the carbonic anhydrase inhibitory capacity of these novel derivatives. Their results also revealed similar findings of good inhibition potential of these new compounds against CAII, CAIX and CAXII supporting the evidence of potential role of morpholine based derivatives as carbonic anhydrase inhibitors [50].

Another aspect of the study was to evaluate the anticancer potential of synthesized ligands. Mouse ovarian cancer cell line ID8 was utilized to examine the inhibition of proliferation of cells. The potential of morpholine based derivatives in ovarian cancer cell line is not studied before. The cell lines are known to express both the carbonic anhydrase IX iso-enzyme as well as hypoxia inducible factor 1α. Due to the low evidence of effect of these derivatives on ovarian cell line the potential of these compounds was studied. The results showed notable inhibition of proliferation of cells by derivative **1h** with 4-fluro aniline moiety showed IC_{50} of 9.4 μM concentration compared to standard cisplatin having IC_{50} of 8.50 μM at similar concentration whereas, compounds **1i** with thymol moiety**, 1l** with amino oxadiazole moiety and **1b** with pyrrolidine moiety also showed good inhibitory potential with IC_{50} of 11.2, 15.6 and 14.8 μM, respectively (Fig. 8). The study for the first time reported the potential of morpholine based derivatives against ovarian cancer cell lines.

To further explore the effectiveness of synthesized compounds, the inhibition potential against the hypoxia-inducible factor 1α was also studied. During hypoxia the overexpression of CAIX is due to the increased HIF-1α activity. Therefore, the effect of synthesized compounds on the inhibition of HIF-1α was studied. The study revealed promising activities of compounds **1b, 1c, 1h** and **1i** as HIF-1α inhibitors. The compound **1b** showed maximum inhibition in comparison to control. The compounds **1h** and **1i** also reported good inhibition, however, compound **1d** showed no significant inhibition in the concentration of HIF-1α. We report for the first time the effect of morpholine derivatives on hypoxia inducible factor -1α showing promising effect of compounds in targeting HIF-1α. The study of chemical structures and *invitro* biological activity of synthesized derivatives **(1a-1n)** revealed that whether it is ca inhibitory activity or anticancer activity or HIF-1α assay, the derivatives with heterocyclic moieties and electronegative substituted aryl ring system possessed promising biological activity then that of simple aryl ring system and non-heterocyclic moieties.

The *in silico* docking analysis and validation docking process were also implemented to validate the binding affinity of compounds on the active binding sites of carbonic anhydrase protein and HIF-1α protein targets. The docking analysis of target protein carbonic anhydrase revealed efficient binding of ligands with highest predictive binding ability. All the ligands showed binding at the active binding site with amino acid ASN11, GLY6, PHE231, HIS4, GLU170, ASN62 and HIS64 as important residues involved in interaction. The similar pattern of interaction was observed with the target protein HIF-1α with all the ligands showing binding in the active binding site of protein. The important amino acid residues showing interaction were ARG165, ASN230, CYS128, GLY216, GLN192, CYS191, TRP215, SER195, VAL213 and GLN80. In conclusion, the study highlighted the important role of morpholine based derivatives as carbonic anhydrase inhibitor, HIF-1α inhibitor as well as possessing the antitumor activity against ovarian cancer. However, further studies, would be required to understand the basic mechanism underlying the inhibition of these processes.

5. Conclusions

In the present work, a succession of some novel synthetic analogs morpholine acetamide derivatives i.e. compounds **(1a-1n)** were exceptionally designed, characterized and analyzed for their anti-tumor potential and carbonic anhydrase inhibitory activity. Molecular docking analysis were also executed to check the binding affinity of the synthesized compound with their targets and epacadostat (inhibitor of CA-IX) was used as standard. Compounds **1c, 1d, 1h** and **1i** exhibited significant *in vitro* carbonic anhydrase inhibition potential whereas compound **1h** demonstrated significant inhibition approximate to acetazolamide practically. Likewise, four of the prepared compounds displayed remarkable anti-tumor potential especially compound **1b, 1c, 1h,** and **1i** exhibited suitable, while derivative **1h** had lower IC_{50} value close to cisplatin when investigated through *in vitro* MTT assay. The studies depict that the new synthetic derivatives can be good future drug candidates.

Statements and declarations

Authors have no conflict of interest to declare whatsoever.

Data availability statement

Data will be made available on suitable request.

CRediT authorship contribution statement

Ahmed Sadiq Sheikh: Data curation, Formal analysis, Investigation, Writing – original draft. **Reem Altaf:** Methodology, Software, Validation, Visualization, Writing – original draft. **Humaira Nadeem:** Conceptualization, Formal analysis, Project administration, Resources, Supervision, Writing – review & editing. **Muhammad Tariq Khan:** Investigation, Validation, Writing – original draft, Writing – review & editing. **Babar Murtaza:** Methodology, Supervision, Visualization, Writing – original draft, Writing – review & editing.

Declaration of competing interest

The authors have declared no conflict of interest whatsoever.

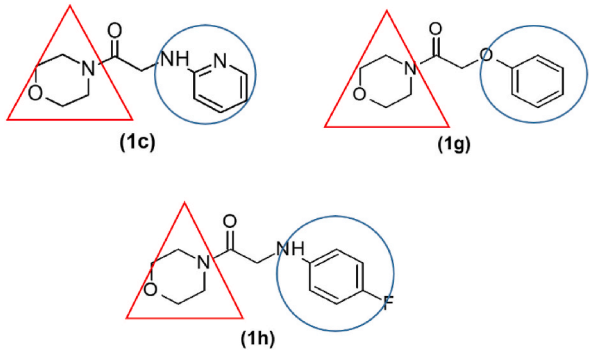

Fig. 7. Structure–activity relationship of **1c**, **1g** and **1h**. The figure indicates morpholine moiety (red triangle) linked with different heterocyclic and aryl amines (blue circle) *via* the amide bond. (For interpretation of the references to colour in this figure legend, the reader is referred to the Web version of this article.)

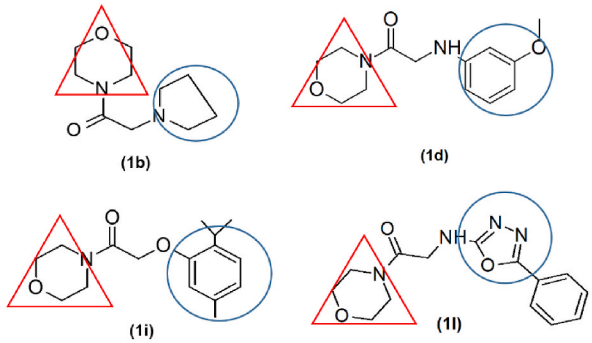

Fig. 8. Structure–activity relationship of **1b**, **1d**, **1i** and **1l**. The figure indicates morpholine moiety (red triangle) linked with different heterocyclic and aryl amines (blue circle) *via* the amide bond. (For interpretation of the references to colour in this figure legend, the reader is referred to the Web version of this article.)

Acknowledgments

We are also grateful to Riphah International University for the provision of research prerequisites.

References

[1] D.O. Ochwang'i, C.N. Kimwele, J.A. Oduma, P.K. Gathumbi, J.M. Mbaria, S.G. Kiama, Medicinal plants used in treatment and management of cancer in Kakamega County, Kenya, J. Ethnopharmacol. 151 (3) (2014) 1040–1055.
[2] P.C. McDonald, J.-Y. Winum, C.T. Supuran, S. Dedhar, Recent developments in targeting carbonic anhydrase IX for cancer therapeutics, Oncotarget 3 (1) (2012) 84.
[3] O. Warburg, On respiratory impairment in cancer cells, Science 124 (1956) 269–270.
[4] J. Welti, S. Loges, S. Dimmeler, P. Carmeliet, Recent molecular discoveries in angiogenesis and antiangiogenic therapies in cancer, J. Clin. Investig. 123 (8) (2013) 3190–3200.
[5] W.R. Wilson, M.P. Hay, Targeting hypoxia in cancer therapy, Nat. Rev. Cancer 11 (6) (2011) 393–410.
[6] V. Alterio, A. Di Fiore, K. D'Ambrosio, C.T. Supuran, G. De Simone, Multiple binding modes of inhibitors to carbonic anhydrases: how to design specific drugs targeting 15 different isoforms? Chem. Rev. 112 (8) (2012) 4421–4468.
[7] T. Dorai, I.S. Sawczuk, J. Pastorek, P.H. Wiernik, J.P. Dutcher, The role of carbonic anhydrase IX overexpression in kidney cancer, Eur. J. Cancer 41 (18) (2005) 2935–2947.
[8] J.P. Kirkpatrick, Z.N. Rabbani, R.C. Bentley, M.E. Hardee, S. Karol, J. Meyer, E. Oosterwijk, L. Havrilesky, A.A. Secord, Z. Vujaskovic, Elevated CAIX expression is associated with an increased risk of distant failure in early-stage cervical cancer, Biomark. Insights 3 (2008) S570. BMI.
[9] A. Scozzafava, C.T. Supuran, Glaucoma and the applications of carbonic anhydrase inhibitors, Carbonic Anhydrase: Mech. Regulation, Links to Dis. Ind. Appl. (2014) 349–359.
[10] C.T. Supuran, A. Scozzafava, Carbonic anhydrases as targets for medicinal chemistry, Bioorg. Med. Chem. 15 (13) (2007) 4336–4350.
[11] Y. Wang, L. Yin, Y. Cui, L. Wang, J. Wu, J. Wang, H. Zhao, C. Liu, Y. Cui, Y. Zhang, Prognostic Significance of Membranous Carbonic Anhydrase IX Expression in Patients with Nonmetastatic Clear Cell Renal Cell Carcinoma of Different Tumor Stages, Cancer biotherapy & radiopharmaceuticals, 2021.
[12] C.T. Supuran, A.D. Fiore, G.D. Simone, Carbonic anhydrase inhibitors as emerging drugs for the treatment of obesity, Expet Opin. Emerg. Drugs 13 (2) (2008) 383–392.
[13] G. De Simone, C.T. Supuran, Antiobesity carbonic anhydrase inhibitors, Curr. Top. Med. Chem. 7 (9) (2007) 879–884.
[14] A. Scozzafava, C.T. Supuran, F. Carta, Antiobesity carbonic anhydrase inhibitors: a literature and patent review, Expert Opin. Ther. Pat. 23 (6) (2013) 725–735.
[15] T. Dorai, I.S. Sawczuk, J. Pastorek, P.H. Wiernik, J.P. Dutcher, The role of carbonic anhydrase IX overexpression in kidney cancer, Eur. J. Cancer 41 (18) (2005) 2935–2947.

[16] J.P. Kirkpatrick, Z.N. Rabbani, R.C. Bentley, M.E. Hardee, S. Karol, J. Meyer, E. Oosterwijk, L. Havrilesky, A.A. Secord, Z. Vujaskovic, Elevated CAIX expression is associated with an increased risk of distant failure in early-stage cervical cancer, Biomark. Insights 3 (2008) S570. BMI.
[17] A. Scozzafava, C.T. Supuran, Glaucoma and the applications of carbonic anhydrase inhibitors, Carbonic Anhydrase: Mech. Regulation, Links to Dis. Ind. Appl. (2014) 349–359.
[18] C.T. Supuran, A. Scozzafava, Carbonic anhydrases as targets for medicinal chemistry, Bioorg. Med. Chem. 15 (13) (2007) 4336–4350.
[19] C. Bahls, M. Fogarty, Reining in a killer disease; cancer and chronic disease in the same sentence? Researchers hope it's not an oxymoron.(News)(Cover Story), Scientist 16 (11) (2002) 16–19.
[20] Y. Li, H. Wang, E. Oosterwijk, Y. Selman, J.C. Mira, T. Medrano, K.T. Shiverick, S.C. Frost, Antibody-specific detection of CAIX in breast and prostate cancers, Biochem. Biophys. Res. Commun. 386 (3) (2009) 488–492.
[21] C.T. Supuran, C. Capasso, The η-class carbonic anhydrases as drug targets for antimalarial agents, Expert Opin. Ther. Targets 19 (4) (2015) 551–563.
[22] J.M.A. Delou, A.S.O. Souza, L.C.M. Souza, Borges H.L. Highlights, In resistance mechanism pathways for combination therapy, Cells 8 (2019), https://doi.org/10.3390/cells8091013.
[23] A.L. Hopkins, Network pharmacology: the next paradigm in drug discovery, Nat. Chem. Biol. 4 (2008) 682–690, https://doi.org/10.1038/nchembio.118.
[24] O.O. Guler, G.D. Simone, C.T. Supuran, Drug design studies of the novel antitumor targets carbonic anhydrase IX and XII, Curr. Med. Chem. 17 (15) (2010) 1516–1526.
[25] S. Pastorekova, M. Zatovicova, J. Pastorek, Cancer-associated carbonic anhydrases and their inhibition, Curr. Pharmaceut. Des. 14 (7) (2008) 685–698.
[26] F.E. Koehn, G.T. Carter, The evolving role of natural products in drug discovery, Nat. Rev. Drug Discov. 4 (3) (2005) 206–220.
[27] R. Altaf, H. Nadeem, U. Ilyas, J. Iqbal, R.Z. Paracha, H. Zafar, A.C. Paiva-Santos, M. Sulaiman, F. Raza, Cytotoxic evaluation, molecular docking, and 2D-QSAR studies of dihydropyrimidinone derivatives as potential anticancer agents, J. Oncol. 2022 (2022), 7715689.
[28] M.B. Buddh, Studies on Some Compounds of Therapeutic Interest, Saurashtra University, 2010.
[29] für die Entwicklung, S. P., Substituted Pyridines for the Development of Novel Therapeutics-Antifungals and Antidiabetics.
[30] O. Bekircan, M. Küxük, B. Kahveci, S. Kolaylı, Convenient synthesis of fused heterocyclic 1, 3, 5-triazines from some n-acyl imidates and heterocyclic amines as anticancer and antioxidant agents, Arch. Pharmazie: Int. J. Pharmaceu. Med. Chem. 338 (8) (2005) 365–372.
[31] R. Narang, B. Narasimhan, S. Sharma, A review on biological activities and chemical synthesis of hydrazide derivatives, Curr. Med. Chem. 19 (4) (2012) 569–612.
[32] G. Yadav, S. Ganguly, Structure activity relationship (SAR) study of benzimidazole scaffold for different biological activities: a mini-review, Eur. J. Med. Chem. 97 (2015) 419–443.
[33] A. Angeli, T.S. Peat, S. Selleri, A.S.A. Altamimi, C.T. Supuran, F. Carta, X-Ray crystallography of epacadostat in adduct with carbonic anhydrase IX, Bioorg. Chem. 97 (2020), 103669.
[34] Shashidhar N. Rao, Martha S. Head, Kulkarni Amit, Judith M. LaLonde, Validation studies of the site-directed docking program LibDock, J. Chem. Inf. Model. (2007) 2159–2171.
[35] M. Al-Rashida, S. Hussain, M. Hamayoun, A. Altaf, J. Iqbal, Sulfa drugs as inhibitors of carbonic anhydrase: new targets for the old drugs, BioMed Res. Int. 2014 (2014).
[36] A. Bahuguna, I. Khan, V.K. Bajpai, S.C. Kang, MTT assay to evaluate the cytotoxic potential of a drug, ♯ Bangladesh J. Pharmacol. 12 (2) (2017) 115–118.
[37] L.-o. Vajrabhaya, S. Korsuwannawong, Cytotoxicity evaluation of a Thai herb using tetrazolium (MTT) and sulforhodamine B (SRB) assays, J. Anal. Sci. Technol. 9 (1) (2018) 1–6.
[38] M. Yasuda, M. Miyazawa, M. Fujita, H. Kajiwara, T. Iida, T. Hirasawa, T. Muramatsu, M. Murakami, M. Mikami, K. Saitoh, Expression of hypoxia inducible factor-1α (HIF-1α) and glucose transporter-1 (GLUT-1) in ovarian adenocarcinomas: difference in hypoxic status depending on histological character, Oncol. Rep. 19 (1) (2008) 111–116.
[39] Freedman, S. J. S. B. F. R. O. C. P. B. h.-i. f.-α. P. N. A. S. U., Sun ZY, Poy F, Kung AL, Livingston DM, Wagner G, and Eck MJ. 2002, vol. 99, 5367-5372.
[40] C.T. Supuran, Carbonic anhydrases: novel therapeutic applications for inhibitors and activators, Nat. Rev. Drug Discov. 7 (2) (2008) 168–181.
[41] C.T. Supuran, Structure and function of carbonic anhydrases, Biochem. J. 473 (14) (2016) 2023–2032.
[42] D. Neri, C.T. Supuran, Interfering with pH regulation in tumours as a therapeutic strategy, Nat. Rev. Drug Discov. 10 (10) (2011) 767–777.
[43] C.T. Supuran, Carbonic anhydrase inhibitors and their potential in a range of therapeutic areas, Expert Opin. Ther. Pat. 28 (10) (2018) 709–712.
[44] C.T. Supuran, Advances in structure-based drug discovery of carbonic anhydrase inhibitors, Expet Opin. Drug Discov. 12 (1) (2017) 61–88.
[45] C.T. Supuran, Carbonic anhydrase inhibition and the management of hypoxic tumors, Metabolites 7 (3) (2017) 48.
[46] R.D. Vaughan-Jones, K.W. Spitzer, Role of bicarbonate in the regulation of intracellular pH in the mammalian ventricular myocyte, Biochem. Cell. Biol. 80 (5) (2002) 579–596.
[47] A. Greijer, P. Van Der Groep, D. Kemming, A. Shvarts, G. Semenza, G. Meijer, M. Van De Wiel, J. Belien, P.J. van Diest, E. van der Wall, Up-regulation of gene expression by hypoxia is mediated predominantly by hypoxia-inducible factor 1 (HIF-1), J. Pathol.: J. Pathol. Soc. Great Britain and Ireland 206 (3) (2005) 291–304.
[48] M. Choschzick, E. Oosterwijk, V. Müller, L. Woelber, R. Simon, H. Moch, P. Tennstedt, Overexpression of carbonic anhydrase IX (CAIX) is an independent unfavorable prognostic marker in endometrioid ovarian cancer, Virchows Arch. 459 (2) (2011) 193–200.
[49] P. Hynninen, L. Vaskivuo, J. Saarnio, H. Haapasalo, J. Kivelä, S. Pastorekova, J. Pastorek, A. Waheed, W. Sly, U. Puistola, Expression of transmembrane carbonic anhydrases IX and XII in ovarian tumours, Histopathology 49 (6) (2006) 594–602.
[50] B. Swain, C.S. Digwal, A. Angeli, M. Alvala, P. Singh, C.T. Supuran, M. Arifuddin, Synthesis and exploration of 2-morpholino-4-phenylthiazol-5-yl acrylamide derivatives for their effects against carbonic anhydrase I, II, IX and XII isoforms as a non-sulfonamide class of inhibitors, Bioorg. Med. Chem. 27 (21) (2019), 115090.